Use of Sedimentary Simulations for Dating Sequence Boundaries and Measuring the Size of Eustatic Sea Level Changes: an Example from the Neogene of the Bahamas

C. G. St. C. Kendall and A. Sen

1 Introduction

Two major problems which confront sequence stratigraphers interpreting seismic lines are (1) the ages of sequence boundaries (Miall 1990); and (2) the size of eustatic sea-level changes (Burton et al. 1988). Sedimentary simulation can be used in conjunction with sequence stratigraphy to interpret seismic cross sections to solve these problems. To this end, a seismic cross section that records the Neogene carbonate fill of the West Andros Channel of the Bahamian Platform was interpreted, and a sedimentary simulation based on empirical modeling reproduced this interpretation. This match between the interpretation and the seismic has enabled the age dating of sequence boundaries and determined that the size of the eustatic sea-level excursions for this time period matches the sea-level events on the Haq et al. (1987) chart.

At the heart of this study is the recognition of eustatic events, evidenced by the presence of synchronous sedimentary sequences and the unconformities that bound them (Vail et al. 1978). These eustatic signals produce changes in the accommodation for sedimentary fill and have a worldwide extent. Their chronostatigraphic correlation is dependent upon reliable time markers spaced sufficiently close in time to bracket the sediment packages formed in response to changes in sea level. The amplitude of these eustatic events presents an enigma, since these cannot be determined independent of models for tectonic behavior and sedimentation. The result is that, while sea-level charts can be created, the amplitudes of given events on these charts are dependent on assumptions concerning the rates of subsidence and sediment accumulation. Unfortunately, there are no direct methods available to measure the amplitudes of sea-level variations. This is because there is no datum available to measure from, since the earth surface constantly moves in response to (1) sediment compaction, (2) isostatic response to sediment loads, and (3) thermal tectonic movement (Burton et al. 1988). Thus, the relative sea level position is dependent on tectonic behavior and eustatic position, so the size of either of these two variables can be measured only by assuming a model for the other's behavior. Methods which attempt to indirectly measure sea level have to assume models of tectonic behavior. Such methods include tide gauges,

strandline position (which additionally assume a continental relief and/or tectonic behavior), paleobathymetry, seismic sequence onlap, stacked subsidence curves, and the matching of sequence geometries with graphical simulations (Burton et al. 1988). Despite the fact that sea-level amplitudes cannot be measured independently, stratigraphic predictions based on sea-level curves or tectonic models of behavior are reproducible and verifiable away from areas of interest. This is because the onlapping or downlapping of the sediments involved is dependent on the rates of sedimentation, the tectonic movement and sea-level position. Hence, if rates of subsidence and of carbonate accumulation are constant for several cycles of eustatic sea level, then the frequency and amplitude of the onlapping sequence geometries will be the product of the frequency and amplitude of the changes in eustatic sea level. The hypothesis presented here is that if the sequence geometries of a sedimentary simulation generated with the Haq et al. (1987) chart match the interpreted sequence on the seismic, then the ages of these latter sequences can be assumed to match those of the simulation. The shallow water carbonate platforms of Bahamas provides a perfect opportunity to test the hypothesis.

2 The Assumptions

To build reasonable simulations of stratigraphic interpretations that capture sea-level events, geologic sections are required for which it can be assumed that there was a low rate of uniform subsidence and a high rate of constant sediment accumulation for several sea-level cycles of the Haq et al. (1987) curve. Examples of the response to this kind of stratigraphic signal can be seen on the seismic sections of the Lower Cretaceous of offshore South Africa (Fig. 1) and the onshore seismic of the National Petroleum Reserve of Alaska (Fig. 8 in Bird et al. 1992). It can also be recognized on the seismic record for the Neogene of the Bahamas platform (Fig. 2) and the Neogene section displayed in the cliffs of the island of Mallorca, offshore eastern Spain (Fig. 3). In all these locations, the rates of subsidence appear to be low while the sedimentation rates are high. The result is that the changing onlapping position of the sequence geometries of these areas are assumed to be produced by sea-level changes.

With the absence of absolute sea-level positions for a paleoshore, it was assumed that should the rate of sedimentation be sufficiently high, then any shoreward accommodation was filled to sea level. When this happens the shelf margin can then be used as a proxy of the sea-level position. This assumption is not unreasonable for most carbonate shelves, but when it is applied to clastics confirmatory paleobathymetric markers are needed. In the case of carbonates the reasonableness of this assumption can be seen expressed in the seismic sections of the Neogene of the Bahamas (Fig. 2) and the cliffs of Neogene sediments exposed in the cliffs of the island of Mallorca (Fig. 3). The sedimentary sections developed in both these locations are the product of carbonate accumulation ‚rates which were high enough to fill the accommodation space up to sea level during

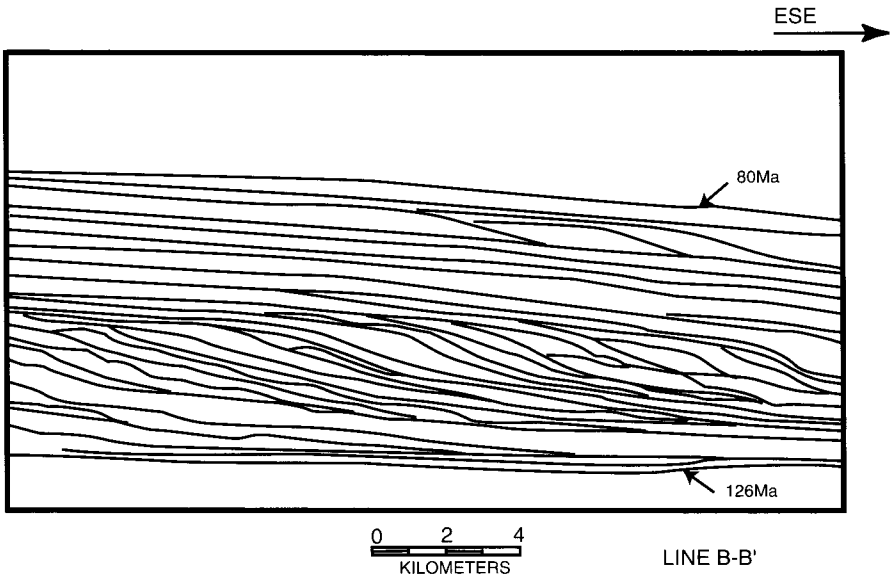

Fig. 1 Part of interpreted seismic section *(line B-B')* of Lower Cretaceous from Southern Platmos subbasin, off-shore South Africa showing prograding clinoform sediment wedges. (After Brown et. al. 1995)

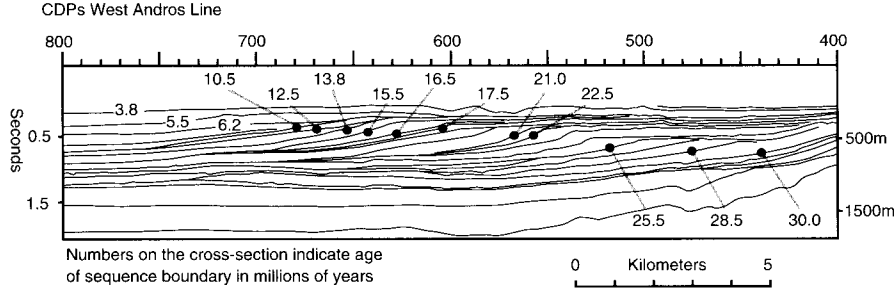

Fig. 2 Interpreted seismic section from the Bahamas

each sea-level cycle. In both cases, the Neogene section is expressed by prograding clinoforms. In the Bahamas, this effect can be seen on both the western side of the bank and in an interior sea, the Straits of Andros (Eberli and Ginsburg 1987, 1989).

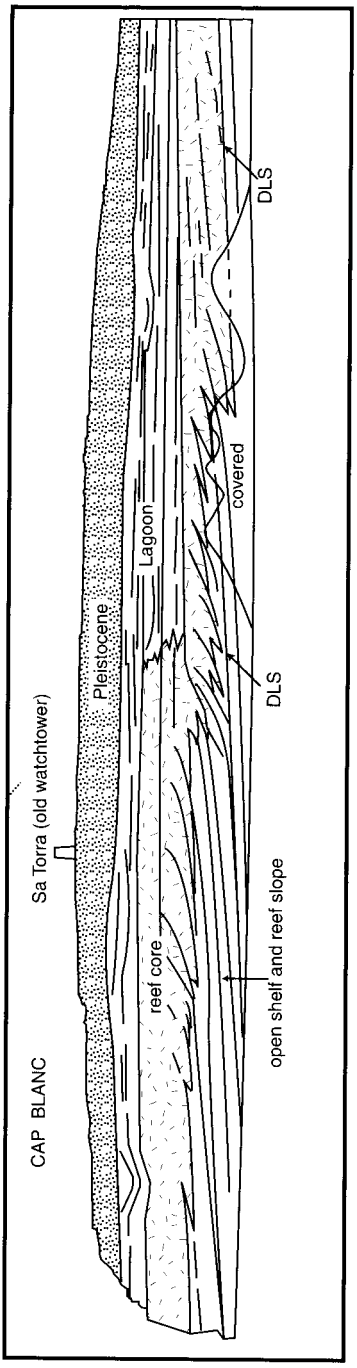

Fig. 3 A schematic map of the Miocene reef complex and Cap Blanc, Spain (CS condensed section; DLS downlap surface). (After Pomar 1993)

3
Sequence Stratigraphy and Simulation of the Andros Channel

3.1
Introduction to the Data Set

The sequence stratigraphy of the Andros Channel involves an interpretation of carbonate platform development, based on seismic data and limited well control from northwestern Great Bahamas Bank (Fig. 4). This Bahamian seismic data set consists of a cross-bank profile (Fig. 2) that was part of an approximately 700-km grid of unmigrated, multichannel seismic profiles. The top 1.7 s (two-way travel time) were used for the study. This seismic profile is tied to the Great Isaac well at the northwestern edge of the Great Bahamas Bank. The time/depth conversion from the Great Isaac well indicates that the entire Cenozoic history is recorded in these upper sections (Tator and Hatfield 1975; Schlager et al. 1988). The cuttings from this well give some of the initial information on the lithology and age of the reflectors (Schlager et al. 1988; Eberli and Ginsburg 1987, 1989). More recently, two continuously cored wells positioned on the cross-bank profile record the Late Miocene-Recent progradation of the margin (Eberli et al. 1994).

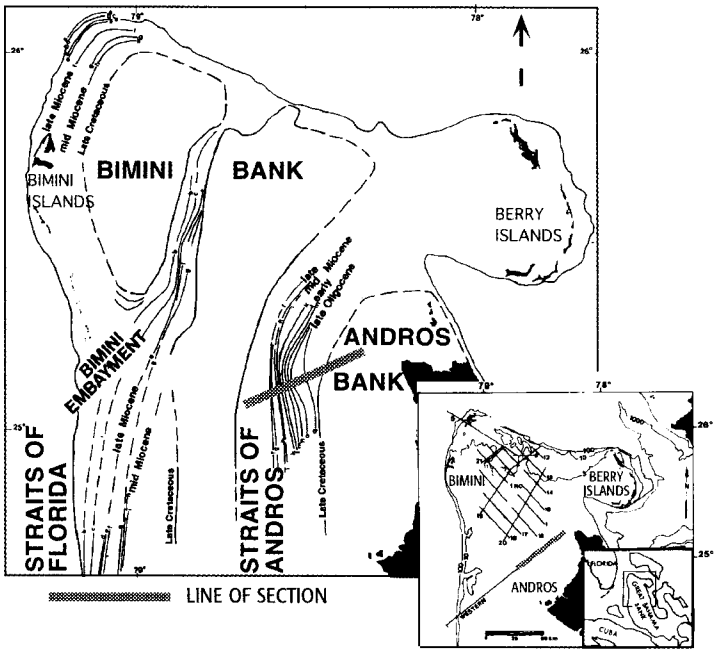

Fig. 4 Map of Great Bahamas Bank showing location of seismic section modeled in this chapter

Seismic profiles of the northwestern Great Bahamas Bank have been interpreted to document the lateral growth potential of isolated platforms that were welded together by margin progradation to form larger banks (Eberli and Ginsburg 1987, 1989). The mechanism responsible for an evolution from aggradation to progradation was thought to be sediment overproduction on the platform (Hine et al. 1981, Willer et al. 1990). Excess sediment was transported offbank and caused a decrease in accommodation space on the marginal slope. Progradation occurred in pulses that are interpreted to result from third-order sea-level fluctuations (Eberli and Ginsburg 1987, 1989). Limited well control has prevented confirmation of these hypotheses, but sedimentary simulation can be used to demonstrate the proposed theory for platform evolution is reasonable, and matches the sea-level events on the Haq et al. (1987) charts (Eberli et al. 1994).

3.2
Seismic Stratigraphic Interpretation

Eberli and Ginsburg (1987) had previously correlated sequence boundaries on the seismic section across the Andros Channel to the Haq et al. (1987) chart. In the present study, the line was re-interpreted. Initially second-order unconformities were identified on the basis of their very extensive erosional character and their correlation to the second-order sea-level events of the Haq et al. 1987 chart (Fig. 5). Third-order unconformities were then identified enclosing their equivalent seismic sequences. The ages of these latter sequences were bracketed with the ages determined from the second-order type 1 unconformities, and correlated with the third-order, type 1, unconformities of the Haq et al. (1987) chart (Fig. 5). As can be seen from the interpretation of the seismic, the major events on the Haq curve have produced distinct stratigraphic signals (Fig. 3). For instance, following the sea-level fall at 30 Ma in early Oligocene times, a major unconformity was created. This separates the Upper Neogene carbonate accumulation from the rest of the Tertiary and the Cretaceous. Similarly, a major fall in sea level occurred at 10.5 Ma and this also has a distinct seismic expression as a major unconformity. It is apparent that the sea level fell below the shelf margin with the resulting unconformity bracketing the series of third-order sea-level events between 10.5 and 30.0 Ma. While examining the geometric position of these latter sequences with respect to the shelf margin, and counting them, it can be seen that more unconformities can be identified than there are sea-level events on the Haq et al. (1987) chart. It is suspected that some of these interpreted sequences may be a result of separating the products of both low and high stand cycles of sea level as sequences. Despite these additional sequences, there appears to be a general match of the onlapping relationship of the different sequences on the seismic (Fig. 2) and the extent of basinward retreat of shorelines, with the amplitude of the sea-level events (Fig. 5). Having made the sequence stratigraphic interpretation, a simulation was developed.

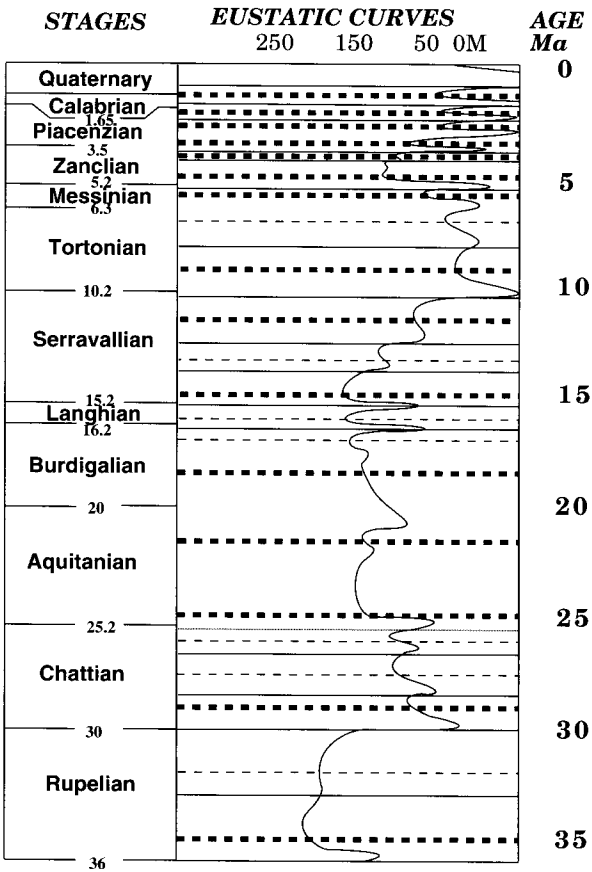

Fig. 5 Chart of Neogene eustatic events from 36 Ma to present. (After Haq et. al. 1987)

3.3 Simulation Input Parameters

Time Interval. The last 30 Ma of platform evolution of the Bahamas/Straits of Andros was modeled using time steps of 250 ka duration. The time taken for the simulation to execute was directly effected by these time steps. A duration of 250 ka produced 120 time steps which were considered essential for the proper resolution of the simulation. (Table 1a)

Initial Basin Surface. The initial depositional surface of the Straits of Andros used in the simulation was derived from the seismic line. This was the sequence boundary which had the interpolated age of 30 Ma (Fig. 2). The time/depth conversion of this surface and the other sequence boundaries above it were deter-

Table 1(a-f) Different inputs parameters used during simulation of Andros Channel (see text for details)

Time interval

a)

Time steps in simulation	
Duration	Number
250	12

Initial basin surface

b)

Distance (km)	Depth (m)
0	-370
18	-370
26	-71
28	-21

Tectonic movement

c)

Subsidence rates (m/Ka) at specified locations as a function of time			
Time (Ma)	Location across the basin in km		
	1.0000	17.0000	30.0000
-30.0	-0.0090	-0.0090	-0.0090
-18.0	-0.0090	-0.0090	-0.0090
-10.0	-0.0090	-0.0090	-0.0090
-06.5	-0.0345	-0.0345	-0.0310
-06.0	-0.0580	-0.0580	-0.0485
-04.0	-0.0567	-0.0567	-0.0470
00.0	-0.0385	-0.0385	-0.0350

Benthic carbonate depostion (BCD) rates

d)

BCD rates (m/Ka) at different depths as a function of times					
Depth (m)	Time in million years				
	-30.00	-17.00	-14.00	-03.00	00.00
-300	0.00	0.00	0.00	0.00	0.00
-200	0.07	0.07	0.06	0.04	0.07
-50	0.07	0.07	0.06	0.04	0.07
-15	0.35	0.35	0.06	0.04	0.35
-00	0.40	0.40	0.06	0.04	0.40

Pelagic carbonate deposition (PCD) rates

e)

Variation in PCD rates (m/Ka) across the basin as a function of time								
Time (Ma)	-30.00	-24.50	-10.50	-10.00	-4.50	-3.50	-2.50	0.00
Rate	0.0280	0.0217	0.0100	0.008	0.008	0.008	0.080	0.080

Carbonate Parameters

f)

Talus/turbidite depositional angle	20°
Percent talus	30%
Percent turbidite	70%
Talus penetration distance	1 m
Turbidite penetration distance	10 m

mined from the velocity profile of the Great Isaac well (Eberli and Ginsburg 1987, 1989). Only the east side of the Straits of Andros basin was considered for the simulation. This basin was initially formed as an asymmetric trough approximately 30 km wide with a depth of approximately 370 m (Table 1b). As the program calculates the area of sediments per column across the basin, the basin was divided into 60 columns of 0.5 km width.

Eustatic Sea Level. The Haq et al. (1987) sea-level curve (Fig. 5) was used for modeling the Bahamas/Straits of Andros dataset. The size of the sea-level excursion directly controlled the high-frequency geometries of the sequences.

Tectonic Movement. The subsidence history of the Bahamian/Straits of Andros dataset was derived directly from the seismic section and was initially modeled by the simulation with no sediment fill. The thickness of the sediment measured on the seismic crossing the platform was used as a first approximation to determine the changes in the rate of subsidence. It can be seen that these rates changed several times through the 30-Ma period, and at different locations across the basin, reflecting low frequency changes in accommodation space at different time intervals as well as different locations. A constant rate of 0.009 m/ka was used for 30 to 10 Ma and faster rates has to be used thereafter in order to ensure that there would be enough space available to accommodate the carbonates as they were generated (Table 1c).

Carbonate Deposition. Benthic carbonate production rates mimic the response to photosynthesis of carbonate-producing organisms. Most of the sediment was produced by organisms that were dependent upon light, so production rates decrease rapidly with increasing water depth (Schlager 1981). The simulation modeled accumulation, not production. This accumulation was modeled as from a combination of benthic and pelagic sources. In the simulation, the resulting geometries were very sensitive to small changes in the accumulation rate with depth and time. Note that the accumulation rate fell rapidly in water deeper than 50 m. (Table 1d)

Pelagic deposition is a critical source of carbonate sediment and comes directly from the water column. In the simulation this pelagic rain is defined as accumulation which varied as a function of time (Table 1e). This rate was used to modulate the progradational fill of the basin by the benthic carbonate, enabling the filling the downslope basin so the progradation could occur. It is believed that in nature this pelagic material included the mud-sized aragonite needles that were transported offbank on the Great Bahamas Bank, probably during highstands of sea level on the banktop (Wilber et al. 1990) and in offbank positions during lowstands.

Carbonate Parameters. As in nature, the simulation limits the growth of carbonate buildup crests to sea level. Excess carbonate accumulation, which would cause the buildups to rise above sea level, was transported off the buildup and deposited as talus and turbidite. The simulation algorithm assumes that all the carbonate talus of the margin came from the "reef" crest. The carbonate parameters were such that the angle of repose was 20°, and the distance of transport of the apron was 1 km for the apron of sediments and 10 km for turbidites (Table 1f). These values were set at the beginning of each simulation run. The percentage of the talus that was transported downslope off the carbonate platform into the basin was an input parameter of 20% (Table 1). By determining the respec-

tive amounts of backreef and talus deposition, windward versus leeward effects were modeled. The angle of repose of 20° was important for deposition of these mass gravity flows. Carbonates have a high angle of repose, which decreases with cohesiveness (Kenter and Schlager 1989).

Experiments with the Simulation. Several experiments were performed in order to fine tune the simulation. Once the shape of the initial basin surface was determined, the elevation of that surface had to be positioned in such a way that at the end of the simulation run there was an exact fit of the sedimentary fill of each of the sequences to the accommodation. Using Haq et al. (1987) sea-level curve as input, this match was dependent upon both subsidence rates and rates of carbonate accumulation. Attempts were made to keep the subsidence constant through several sea-level cycles. Ultimately a value of 0.009 m/1000 years was selected and this value was kept constant from 30–10 Ma. Thereafter, the subsidence rate had to be increased, especially after 6 Ma, to enable the exact fill of sediments for that time interval. Additionally erosional surfaces were created at the interpreted type 1 sequence boundaries of 10.5 and 3.5 Ma. These erosional events are obvious on the seismic and the 3.5 Ma boundary has a particularly irregular erosional surface.

Once subsidence was determined, the rate of benthic carbonate accumulation and that of pelagic deposition were established individually and coordinated with each other. Then two sets of experiments were performed. In one, the benthic carbonate rates were varied with a constant rate of pelagic accumulation, and in another, with slightly different constant values of benthic carbonate rates, the rate of pelagic accumulation was changed. In each case the resulting simulation was matched step by step with the seismic interpretation.

Though the rates of accumulation for pelagic and benthic carbonate rates were varied considerably, the experiments showed that once a combination of the two sources of carbonate produced the best match between the simulation and seismic, it was very difficult, if not impossible to further change the rates to produce better matching simulation outputs. This combination of benthic and pelagic rates produced the correct dimensions for the progradation and aggradation of the sediment wedges without oversteepening the prograding clinoforms. The timing and sequences of progradation was controlled by the size and timing of the sea-level excursions. Attempts were also made to develop similar geometries, with different sea-level curves and different values of same input parameters. While it was possible to produce similar geometries it was, however, not possible to match the output to the seismic interpretation.

3.4
Results from the Bahamas Simulation Execution

When the simulation is examined in detail, it is possible to see that each one of the sequences produced, matches those on the seismic (Fig. 6). These are in order, sequences from 30 to 28.5 Ma 28.5 to 25.5 Ma; from 25.5 to 22.5 Ma; from 22.5 to 21 Ma; from 21 to 17.5 Ma; from 17.5 to 16.5 Ma; from 16.5 to 15.5 Ma;

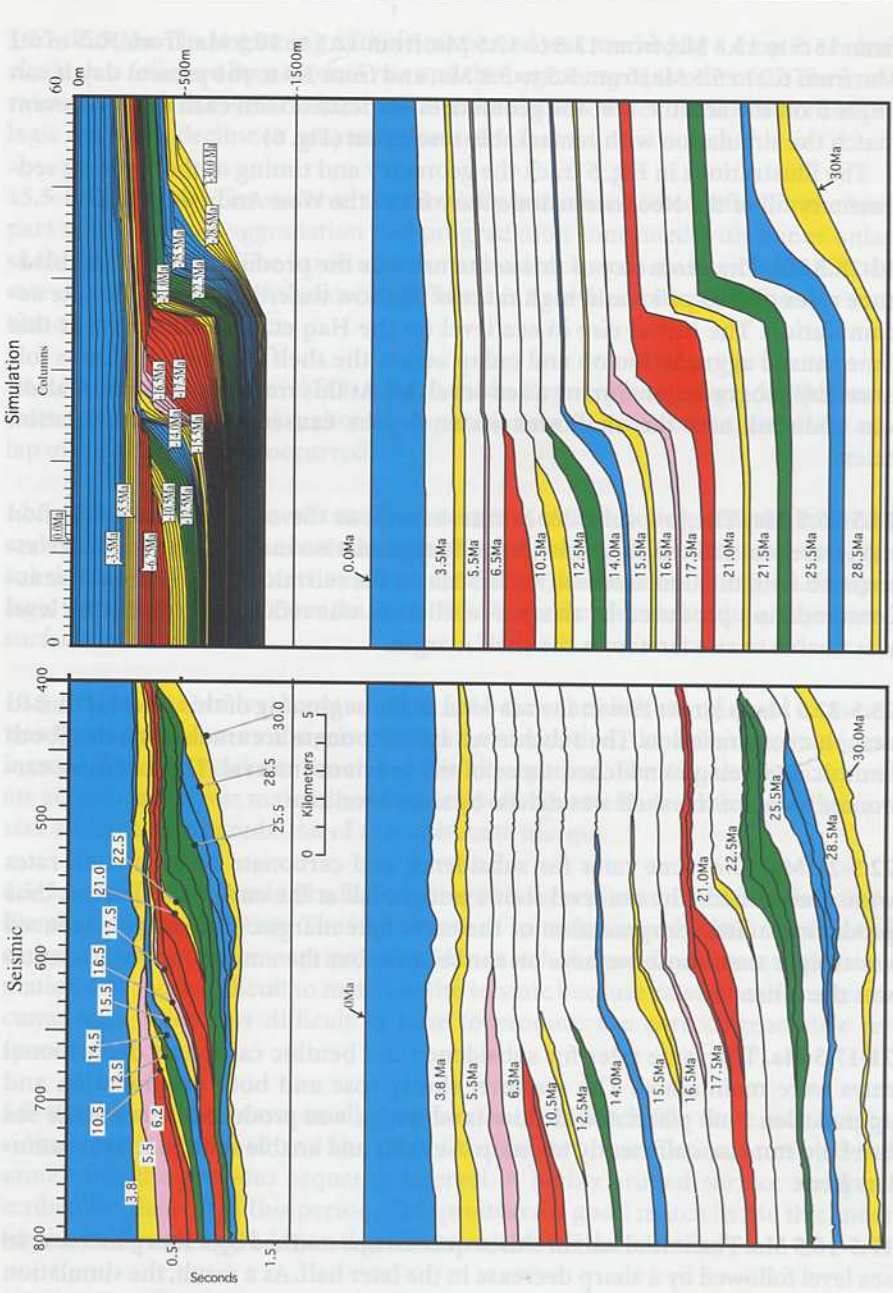

Fig. 6 Comparison of the simulation with the seismic for individual sequences. Each *date* indicates the age of the boundary above and below it (except for 30 and 0 Ma). Time steps shown in the main simulation are removed later for clarity. See text for details

from 15.5 to 13.8 Ma; from 13.8 to 12.5 Ma; from 12.5 to 10.5 Ma; from 10.5 to 6.2 Ma; from 6.2 to 5.5 Ma; from 5.5 to 3.8 Ma; and from 3.8 to the present day. It can be seen on the seismic that the geometries associated with each sea level event match the simulation with remarkable resolution (Fig. 6).

The illustrations in Fig. 6 track the geometry and timing of the evolving sedimentary fill of the Neogene sedimentary fill of the West Andros channel.

30-28.5 Ma. The geometry of this sequence was the product of the low subsidence rates of 0.09 m/ka and high rates of shallow water benthic carbonate accumulation. The initial rise in sea level on the Haq et.al. (1987) chart at this time caused aggradation on and onlap across the shelf margin which was followed by progradation during a sea-level fall. At this time the accommodation was reduced, and the shallower water depths caused faster accumulation rates.

28.5-25.5 Ma. The low subsidence rate, as well as the carbonate accumulation rate, were maintained. Aggradation and progradation matched the sequence associated with the time interval 30-28.5 Ma on the seismic interpretation. The accommodation produced by this sea-level event was reduced, since the sea level was unable to rise far across the shelf margin.

25.5-22.5 Ma. A larger rise in the sea level at the beginning of this interval caused carbonate aggradation. The subsidence and carbonate accumulation rates (both benthic and pelagic) matched those of the previous interval. The extensive carbonate onlap of the shelf was driven by a sea-level rise.

22.5-21 Ma. The same rates for subsidence and carbonate accumulation rates were maintained. The sea level shows a slight fall at the end of this period, thus producing a little progradation of the carbonate margin. The ramps produced are steeper than those we have on the seismic, but the amount of progradation was the same.

21-17.5 Ma. The same rates for subsidence and benthic carbonate depositional rates were maintained. The sea level slowly rose and both progradation and aggradation took place. A wide lowstand wedge was produced, because the sea level did not rise sufficiently to onlap the shelf and enable sediment to accumulate here.

17.5-16.5 Ma. The initial half of this sequence was marked by a sharp increase in sea level followed by a sharp decrease in the later half. As a result, the simulation shows an aggradation and onlap of the shelf followed by progradation. The same rates for subsidence was maintained. The deep water benthic carbonate rate remained the same, but the shallow water rate started to decline. The basin was too deep for much progradation to take place, and this also produced a steeper ramp.

16.5- 15.5 Ma. The beginning of this time period was marked by a drop in sea level which is followed by a marked rise and the beginning of another fall. The same rates of subsidence were maintained, and the shallow water benthic as well as pelagic showed a decline in accumulation rate.

15.5-14 (13.8) Ma. The sea level rose initially but remained constant in the later part of this period, aggradation and progradation continued with minor onlap of the shelf margin. The same rates for subsidence were maintained, while the rate of accumulation of shallow water benthic as well as pelagic carbonate continued to steadily decline.

14 (13.8)-12.5 Ma. Sea-level falls caused the basin margin to prograde. The same rates for subsidence and carbonate depositional rates were maintained. No onlap of the shelf margin occurred.

12.5-10.5 Ma. The sea level remained constant before falling drastically at the end of this sequence. The basin margin showed progradation. The same rates for subsidence and benthic carbonate accumulation rates were maintained. The pelagic rate dropped to 0.008 m/ka. The 10.5 Ma surface is marked by an erosional surface.

10.5-6.5 Ma. The sea level continued to fall below the shelf margin and to maintain the match between the seismic and the simulation, the subsidence rate was increased to –0.03 m/ka at the end of this time period. The same rate of carbonate accumulation was maintained to fill the offshore basin and maintain the correct amount of progradation of the carbonate margin.

6.5-5.5 Ma. The sea level fell a little during this interval and extended the ramp-like shallow progradation. The higher rate of subsidence and similar low rate of carbonate accumulation was maintained to match the previous interval, the simulation was more difficult to match to the seismic because rates of carbonate accumulation were now difficult to tune to produce the correct geometric response.

5.5-4(3.8) Ma. There was a small, gradual rise in sea level. The same rate of subsidence was maintained and the rate of carbonate accumulation remained the same as in the previous sequence interval. A highly eroded surface was prescribed for the end of this period. This produced a good match in the thickness for the onlap and aggradational geometries seen on the seismic.

4(3.8)-0 Ma. The thickness or the final basin fill of the shelf was obtained by keeping the rate of subsidence constant while increasing the rates of pelagic and benthic carbonate accumulation. The pelagic accumulation rate was increased to 0.08 m/ka while the shallow water benthic rates returned to the initial high values.

4 Discussion and Conclusions

The laterally stacked sequences of a seismic section are the product of sea-level changes whose signal can be identified by making a sequence stratigraphic interpretations (Vail et al. 1988). As Eberli et al. (1994) showed earlier a sedimentary simulation can successfully reproduce the geometries seen on a seismic line. The seismic data documents the fill of the Straits of Andros and the sediments are expressed as a series of onlapping and downlapping wedges with various angles of slope. The simulation output produces a match with the seismic interpretation. The simulation helped to quantify individual factors controlling aggradation and progradation in the Bahamas. It showed that different basin depths effected the timing and extent of progradation. It also showed that there was a close balance between aggradation and progradation, and that small changes in the rate of relative sea-level movement and/or carbonate accumulation rates caused immediate switches from aggradation to progradation of the margin. Progradation took place after the space on the upper slope had been reduced and the sediment transported offbank could fill the remaining space and extend the platform margin farther basinward. In particular, progradation was triggered by sea-level drops that shifted sediment production and accumulation to the margin slope. Carbonate production rates similar to modern rates were required to produce the sediment necessary for progradation, which suggests that carbonate production has been consistently high since the early Tertiary. At the same time, repeated exposure and erosion have reduced the overall preservation and decreased the overall accumulation rate.

Thus, progradation occurred in pulses which are recorded on the seismic lines and are confirmed by the simulation as a succession of prograding and sigmoidal sequences, with each sigmoid believed to have been formed as the result of a single cycle of sea-level fall and rise (Eberli and Ginsburg 1989). Each prograding sequence was up to 500 m thick and probably consisted of an offlapping complex of reefal carbonates covered by calcareous sand. Eberli and Ginsburg (1989) thought that during the transgressive stages, marginal reefs were established and then buried during the subsequent highstand, when abundant sediment was produced on the flooded bank and transported to and off the leeside of the bank. Their interpretation was based on findings from the leeside of the modern bank where early Holocene reefs are covered by offbank transported sand (Hine et al. 1981). The two 1990 core borings on the western margin of the Great Bahamas Bank have confirmed this interpretation. This justified the use of benthic accumulation as well as a background pelagic rain to produce the geometries during simulation. Interestingly the simulation suggested progradation of the bank margin continued at sea-level lows when the platform was exposed.

For a carbonate shelf setting with a low rate of subsidence and a high rate of sedimentation, a very clear stratigraphic signal is produced by a particular sea-level curve. This requires that the rate of carbonate sedimentation was such that

the accommodation was filled to sea level so that the sediment surface on the shelf can be taken as a proxy of sea level.

For such a case it can be concluded that when the rates of subsidence and carbonate accumulation were constant during several sea-level cycles, a match in the frequency and amplitude of the onlapping geometries of seismic and simulation suggest that the frequency and amplitude of eustatic events of the Haq et al. (1987) input curve is close to reality. This example from Bahamas appears to prove that this is true for the Neogene.

The encouraging results of this simulation of a carbonate platform suggest that simulations should be performed for other areas to see if cross sections can be reproduced. Indeed, having established the dimensions of the events on the Haq sea-level chart, we plan to make a simulation study of the Neogene clastic fill of the Baltimore Canyon. So far, the resulting simulation matched the seismic interpretation of Greenlee et al. (1992), and confirmed the ages of sequence boundaries and so determined the size of local tectonic events.

The Haq eustatic chart might also be used as an input to simulate interpreted cross sections of mixed carbonate/clastic fills. We are considering simulating the early Cretaceous of the Neuquen Basin of Argentina. In this case, with all the control variables undetermined, a complex mix of varying rates of sedimentation, and tectonics are expected to produce a match between the simulation and this cross-section.

Acknowledgments

We would like to acknowledge John Reistroffer and Parvita Siregar for their initial interpretations of the seismic cross section. Dan Gill is acknowledged for his critical reviews of the manuscript. We sincerely thank Chris Crescini and Kurt Johnston for their thoughtful criticism and discussion, Charlton Purvis and Jay Gardner for system maintenance and My Tran for helping in preparation of the text.

References

Bird, Kenneth J. and Molenaar, M. C., 1992, The North Slope Foreland Basin, Alaska: in R. W. Macqueen and D. A. Leckie eds., Foreland Basins and Fold Belts, American Association of Petroleum Geologists, Memoir 55, p.3–363–393.

Brown, L. F., Benson, J. M., Brink, G. J., Doherty, S., Jollands, A., Jungslager, E., H. A., Keenan, J. H. G., Muntingh, A., and Van Wyk, N. J, .S., 1995, American Association of Petroleum Geologists Studies in Geology 41, 184 pages.

Burton, R., Kendall, C. G. St. C., and Lerche, I., 1987, Out of our depth: on the impossibility of fathoming eustasy from the stratigraphic record: Earth Science Reviews, v. 24, p.237–277.

Eberli, G. P. and Ginsburg, R. N., 1987, Segmentation and coalescence of platforms, Tertiary, NW Great Bahama Bank: Geology, v. 15, p. 75–79.

Eberli, G. P. and Ginsburg, R. N., 1989, Cenozoic progradation of NW Great Bahama Bank – A record of lateral platform growth and sea level fluctuations: SEPM Special Publication 44, p. 339–355.

Eberli, Gregor P., Whittle, G. L., Kendall, C. G. St. C., Cannon, R. L., and Moore, P. D., 1994, Testing a seismic interpretation of the great Bahama bank with a computer simulation: American Association of Petroleum Geologists Bulletin, v. 78, p. 981–1004.

Greenlee, S. M., Devlin, W. J., Miller, K. G., G. S. Mountain, and P. B. Flemings, 1992, Integrated sequence stratigraphy of Neogene deposits, New Jersey continental shelf and slope: comparison with the Exxon model,: GSA Bull., v. 104, p. 1403–1411.

Haq, B. U., Hardenbol, J., and Vail, P. R., 1987, Chronology of fluctuating sea levels since the Triassic (250 million years ago to present): Science, v. 235, p. 1156–1167.

Hine, A.C., Wilber, R.J., Bane, J. M., Neumann, A. C., and Lorenson, K. R., 1981, Offbank transport of carbonate sands along open, leeward bank margins: northern Bahamas: Marine Geology, v. 42, p. 327–348.

Kenter, J.A.M., And Schlager, W.,1989, Comparison of shear strength in calcareous and siliciclastic marine sediments: Marine Geology, v.88, p. 145–152.

Miall, A. D., 1990, Principles of sedimentary basin analysis: Springer-Verlag, New York, NY, 668 pages.

Pomar, L., 1993, High-resolution sequence stratigraphy in prograding Miocene carbonates: Application to seismic interpretation: in R. G. Loucks and J. F. R. Say, eds., Carbonate Sequence Stratigraphy, American Association of Petroleum Geologists, Memoir 57, p.389–407.

Schlager, W.,1981, The paradox of drowned reefs and carbonate platforms: Geol. Soc. Amer. Bulletin, v. 92, p. 197–211.

Schlager, W., Bourgeois, F., Mackenzie, G. and Smit, J., 1988, Boreholes at Great Isaac and Site 626 and the history of the Florida Straits. In Austin, J.A.,Jr., Schlager, W., et al., Proc. ODP, Sci. Results, 101, College Station, TX. (Ocean Drilling Program) p. 425–437.

Tator, B.A., And Hatfield, L.E., 1975, Bahamas present complex geology: Oil and Gas Journal, v. 73, p. 172–176.

Vail, P. R., 1988, Seismic stratigraphy interpretation procedure. In: "Atlas of Seismic Stratigraphy", Bally A.W. (ed.), Am. Assoc. Petrol. Geol. Studies in Geology, v. 27, p. 1–10.

Vail, P. R., Mitchum Jr., R. M., Todd, R. G., Widmier, J. M., S. Thompson III, J.B. Sangree, J. B., Bubb, J. N., and Hatlelid, W. G., 1977, Seismic stratigraphy and global changes of sea level. in C.E. Payton ed., Seismic Stratigraphy – Applications to hydrocarbon exploration. American Association Petroleum Geologists Mem. 26; p. 49–212.

Wilber, R. J., Milliman, J. D., and Halley, R. B., 1990, Accumulation of Holocene banktop sediment on the western margin of Great Bahama Bank: Modern progradation of a carbonate megabank: Geology, v. 18, p. 970 – 975.